TRANSVERSE SHEAR AND NORMAL DEFORMATION THEORY FOR VIBRATION ANALYSIS OF CURVED BANDS

BÉLA KOVÁCS
Institute of Mathematics, University of Miskolc
3515 Miskolc-Egyetemváros, Hungary
`matkb@gold.uni-miskolc.hu`

Dedicated to Professor József FARKAS on the occasion of his seventy-fifth birthday

Abstract. A new laminate model is presented for the dynamic analysis of laminated curved bands. The collocation curved band is used to denote a cylinder panel in the plane strain state. The differential equations which govern the free vibrations of a curved band and the associated boundary conditions are derived by Hamilton's principle considering bending, shear and normal deformation of all layers. The author used a new iterative process to successively refine the stress/strain field in the sandwich curved band. The model includes the effects of transverse shear and rotary inertia. The iterative model is used to predict the modal frequencies and damping of simply supported sandwich curved band. The solutions for a three-layer curved band are compared to a three-layer approximate model.

1. Introduction

Laminated composite curved beams have been used in engineering applications for many years. Design applications of isotropic and curved bars, rings and arches of arbitrary shape are assisted by a well-developed theory and proven design guidelines $[1-4]$. The development of the theory and design guidelines for composite curved beams is much less satisfactory. Earlier works are related to sandwich beams or closed composite rings $[5-9]$. The finite element method was used to study the dynamic response of sandwich curved beams by Ahmed $[5-6]$. Free and forced vibrations of a three-layer damped ring were investigated by Di Taranto [7]. Lu and Douglas [8] investigate the damped three-layered sandwich ring subjected to a time harmonic radially concentrated load. The paper gives an analytical solution for the mechanical impedance at an arbitrary point on the surface of the damped structure as a function of the forcing frequency. Furthermore, an experimental procedure is employed to measure the driving point mechanical impedance as a verification of the calculated

results. Transient response was studied for three-layer closed rings by Sagartz [9]. Damping properties of curved sandwich beams with viscoelastic layer were studied by Tatemichi et al. [10]. Viscoelastic damping in the middle core layer was emphasized.

Nelson and Sullivan [11] analyzed the complete circular ring consisting of a layer soft viscoelastic material sandwiched between two hard elastic layers. The equations which govern the forced vibration of a damped circular ring were solved by the method of damped forced modes. The essence of the damped forced mode method is the use of harmonic forcing functions which are in-phase with local velocity and proportional to local inertia loads. The constant of proportionality is the loss factor of the composite structure, η_n. A clear alternative to a damped forced mode solution is to set all the forcing functions to zero and solve the resulting complex eigenvalue problem. Isvan and Nelson [12] investigated the natural frequencies and composite loss factors of free vibration of a soft cored circular arch simply supported at each end. Although harmonic motion is assumed, what is not stated is that some harmonic excitation is required to maintain such motion in the presence of damping. The dynamic eigenvalue problem is then posed for an unforced system. Kovacs [13] solved the problem of free vibrations of a stiff cored sandwich circular arch. All the tangential displacement components are assumed to be piecewise linear across the thickness, thus implying the inclusion of shear deformations and rotary inertia.

The incremental equations of motion based on the principle of virtual displacements of a continuous medium are formulated using the total Lagrangian description by Liao and Reddy [14]. They developed a degenerate shell element with a degenerate curved beam element as a stiffener for the geometric non-linear analysis of laminated, anisotropic, stiffened shells. Bhimaraddi et al. [15] presented a 24-d.o.f. of isoparametric finite element for the analysis of generally laminated curved beams. The rotary inertia and shear deformation effects were considered in this study. Qatu developed a consistent set of equations for laminated shallow [16] and deep arches [17] . Exact solutions are presented for laminated arches having general boundary conditions by Qatu and Elsharkawy [18]. The in-plane free vibrational analysis of symmetric cross-ply laminated circular arches is studied by Yildirim [19] . The free vibration equations are derived based on the distributed parameter model. The transfer matrix method is used in the analysis. The rotary inertia, axial and shear deformation effects are considered in the Timoshenko analysis by the first-order shear deformation theory. Vaswani, Asnani and Nakra [20] derived a closed form solution for the system loss factors and resonance frequencies for a curved sandwich beam with a viscoelastic core by the Ritz method. Rao and He [21] used the energy method and Hamilton's principle to derive the governing equation of motion for the coupled flexural and longitudinal vibration of a curved sandwich beam system. Both shear and thickness deformations of the adhesive core are included. Equations for obtaining the system modal loss factors and resonance frequencies are derived for a system having simply supported ends by the Ritz method.

It is well-known that the accurate determination of the stress field in the laminate configurations is particularly important for 'stress critical' calculations such as damping and delamination. Zapfe and Lesieutre [22] developed an iterative process to

refine successively the shape of the stress/strain distribution for the dynamic analysis of laminated beams. The iterative model is used to predict the modal frequencies and damping of simply supported beams with integral viscoelastic layers.

The eigenproblem of the plane bending of circular arch shaped layered beams was investigated by using the finite element method [23]. The finite element model of the structure has two-two elements along the face thickness and three elements along the thickness of the core. The two edges of the circular arch are simply supported. The corresponding model is formed by eight node hexahedron elements (280 pcs.).

Flexure of the three-layer sandwich arch results in energy dissipation due to strains induced in the viscoelastic layer. In a symmetrical arrangement with identical elastic layers, most of the damping is due to shear of the viscoelastic layer. In an unsymmetrical arrangement, with dissimilar elastic layers, one might expect damping due to direct strain as well as shear in the viscoelastic layer, the former being known as extensional damping and the latter as shear damping. Both these effects have been included by Kovacs [24]. However, the stress-strain law assumed for the viscoelastic layer was not strictly correct and was only an approximation if extensional effects were considered. An analysis of the vibration of transversely isotropic beams, which have small constant initial curvature was presented in Rossettos [25], Rossettos and Squires [26]. A closed-form general solution to the governing equations was derived. Natural modes and frequencies were determined for both clamped and simply supported end conditions. In Khdeir and Reddy [27], an analysis of the vibration of slightly curved cross-ply laminated composite beams is presented. Hamilton's principle is used to derive the equations of motions of four theories. Exact natural frequencies are determined for various end conditions using the state space concept. The combined effects of initial curvature, transverse shear deformation, orthotropicity ratio, stacking sequence and boundary conditions are evaluated and discussed. Yildirim [28] offers a comprehensive analysis of free vibration characteristics of symmetric cross-ply laminated circular arches vibrating perpendicular to their planes. Governing equations of symmetric laminated circular arches made of a linear, homogeneous, and orthotropic material are obtained in a straightforward manner based on the classical beam theory. The transfer matrix method is used for the free vibration analysis of the continuous parameter system.

The present research offers a new laminated model for the dynamic analysis of laminated curved bands, which includes both transverse shear and transverse normal effects. The differential equations which govern the free vibrations of a curved band and the associated boundary conditions are derived by Hamilton's principle considering bending, shear and normal deformation of all layers. The author used a new iterative process to successively refine the stress/strain fields in the sandwich band. The model includes the effects of transverse shear and rotary inertia. The current model is developed for the specific case of a simply supported curved band with uniform properties along the length.

2. Governing equations of motion

The geometry of interest and the notations used are shown in Figure 1. As indicated in the Figure, the curved band ends are simply supported. The collocation curved band is used to denote a cylinder panel in the plane strain state. Consider the curved band with a cylinder middle surface and the radius of curvature R of the middle surface. The curved band consists of three different layers of homogeneous materials bonded together to form a composite structure. Subscript i, where $i = 1, 2, 3$ is used to denote quantities in the various layers, starting from the outermost layer, so that layers 1,3 represent the elastic layers while layer 2 represents the viscoelastic layer. A state of plane strain is assumed, as well as the fact that the materials in each layer of the band are homogeneous and isotropic. Perfect bonding of the layers and linear elasticity are also assumed in the analysis. The composite band is lightly damped and it is assumed that all the energy dissipated is dissipated in the viscoelastic layer.
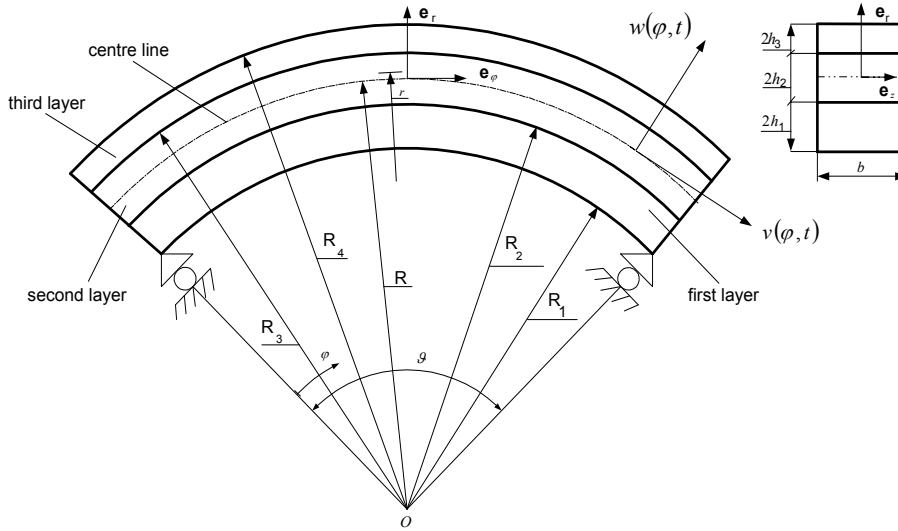

Figure 1. Geometry of the laminated curved band

The form of the displacement field over the domain of the curved band is

$$\mathbf{t}(r, \varphi, t) = u(r, \varphi, t)\mathbf{e}_\varphi + w(r, \varphi, t)\mathbf{e}_r =$$

$$= \left[v_0(\varphi, t) - \frac{r - R}{R} \left(\frac{\partial w_0}{\partial \varphi} - v_0(\varphi, t) \right) + f(r)v_1(\varphi, t) \right] \mathbf{e}_\varphi + [w_0(\varphi, t) + g(r)w_1(\varphi, t)] \mathbf{e}_r$$

$$(2.1)$$

where $f(R) = 0$ and $g(R) = 0$, so (v_0, w_0) denote the displacement of a point (R, φ) of the centre-surface along the circumferential and radial directions, respectively.

The terms $f(r)v_1(\varphi, t)$ and $g(r)w_1(\varphi, t)$ can be thought to be correction to account for transverse shear and normal deformation effects, respectively. The functions $f(r)$ and $g(r)$ represent the shape of the corrections through the thickness of the curved

band, while $v_1(\varphi, t)$ and $w_1(\varphi, t)$ determine its distribution along the circumferential direction. The solution of a given problem requires the determination of the unknown functions $v_0(\varphi, t), v_1(\varphi, t), w_0(\varphi, t), w_1(\varphi, t), f(r)$ and $g(r)$. By using the standard expressions

$$\mathbf{t} = w\mathbf{e}_r + u\mathbf{e}_\varphi, \quad \varepsilon_\varphi = \frac{1}{r}\frac{\partial u}{\partial \varphi} + \frac{w}{r}, \quad \gamma_{r\varphi} = \frac{1}{r}\frac{\partial w}{\partial \varphi} + \frac{\partial u}{\partial r} - \frac{u}{r}, \quad \varepsilon_r = \frac{\partial w}{\partial r},$$

the strain tensor of each layer can be computed from equations (2.1):

$$\varepsilon_\varphi = \frac{1}{r}\left[\frac{\partial v_0}{\partial \varphi} - \frac{r-R}{R}\left(\frac{\partial^2 w_0}{\partial \varphi^2} - \frac{\partial v_0}{\partial \varphi}\right) + f(r)\frac{\partial v_1}{\partial \varphi} + w_0 + g(r)w_1(\varphi, t)\right], \quad (2.2)$$

$$\gamma_{r\varphi} = \left[\frac{df}{dr} - \frac{f(r)}{r}\right]v_1(\varphi, t) + \frac{g(r)}{r}\frac{\partial w_1}{\partial \varphi}, \quad (2.3)$$

$$\varepsilon_r = \frac{dg}{dr}w_1(\varphi, t), \quad (2.4)$$

where

$$f(r) = \left\{\begin{array}{lll} f_1(r) & if & R_1 \leq r \leq R_2 \\ f_2(r) & if & R_2 \leq r \leq R_3 \\ f_3(r) & if & R_3 \leq r \leq R_4 \end{array}\right\}$$

and

$$g(r) = \left\{\begin{array}{lll} g_1(r) & if & R_1 \leq r \leq R_2 \\ g_2(r) & if & R_2 \leq r \leq R_3 \\ g_3(r) & if & R_3 \leq r \leq R_4 \end{array}\right\}$$

are single-valued functions defined at each point through the thickness.

From equation (2.3), it can be seen that the functions $\frac{df}{dr} - \frac{f}{r}$ and $\frac{g}{r}$ represent the shape of the transverse shear strain field through the thickness of the curved band at a given φ-location. While the assumed form of the functions, $f(r)$ and $g(r)$ changes from one iteration to the next, at any given iteration they can be treated as known functions.

The curved band vibrates in the $r\varphi$-plane. It is assumed that the plane strain state occurs within the structure and thus within each i-th layer. By treating the problem as a plane strain one and assuming that the materials in each layer are homogeneous and isotropic, we have the following stress-strain relations:

$$\sigma_{ri} = \frac{E_i}{(1 - 2\nu_i)(1 + \nu_i)}((1 - \nu_i)\varepsilon_{ri} + \nu_i\varepsilon_{\varphi i}), \quad (2.5)$$

$$\sigma_{\varphi i} = \frac{E_i}{(1 - 2\nu_i)(1 + \nu_i)}((1 - \nu_i)\varepsilon_{\varphi i} + \nu_i\varepsilon_{ri}), \quad (2.6)$$

$$\tau_{r\varphi i} = G_i\gamma_{r\varphi i}, \quad (2.7)$$

where E_i is the Young's modulus and G_i is the shear modulus within the i-th layer of the structure. Also ν_i is the Poisson's coefficient, which characterises the compression in the radial direction due to tension in the circumferential direction, and vice versa. In addition the stresses $\tau_{\varphi zi}, \tau_{rzi}$ are equal to zero.

The strain energy stored in the curved band is given by:

$$U = \frac{b}{2} \sum_{i=1}^{3} \int_{\varphi=0}^{\vartheta} \int_{R_i}^{R_{i+1}} \left[\sigma_{ri} \varepsilon_{ri} + \sigma_{\varphi i} \varepsilon_{\varphi i} + \tau_{r \varphi i} \gamma_{r \varphi i} \right] r dr d\varphi \ . \tag{2.8}$$

The kinetic energy, which includes components associated with transverse, in plane and rotary inertia, is given by

$$T = \frac{b}{2} \sum_{i=1}^{3} \int_{\varphi=0}^{\vartheta} \int_{R_i}^{R_{i+1}} \rho_i \left(\dot{\mathbf{t}}_i \right)^2 r dr d\varphi \ , \tag{2.9}$$

where the dots over $\mathbf{t}_1$, $\mathbf{t}_2$ and $\mathbf{t}_3$ denote the partial derivative with respect to time. The differential equations of motion and boundary conditions are derived using Hamilton's principle. The equations of motion for the four unknown functions, $w_0(\varphi, t)$, $w_1(\varphi, t)$, $v_0(\varphi, t)$ and $v_1(\varphi, t)$ are

$$A_{11} \frac{\partial^4 w_0}{\partial \varphi^4} + A_{12} \frac{\partial^2 w_0}{\partial \varphi^2} + A_{13} \frac{\partial^3 v_0}{\partial \varphi^3} + A_{14} \frac{\partial^3 v_1}{\partial \varphi^3} + A_{15} \frac{\partial v_0}{\partial \varphi} + A_{16} \frac{\partial v_1}{\partial \varphi} + A_{17} \frac{\partial^2 w_1}{\partial \varphi^2} +$$

$$+ A_{18} w_0 + A_{19} w_1 = D_{11} \frac{\partial^4 w_0}{\partial \varphi^2 \partial t^2} + D_{12} \frac{\partial^3 v_0}{\partial \varphi \partial t^2} + D_{13} \frac{\partial^3 v_1}{\partial \varphi \partial t^2} + D_{14} \frac{\partial^2 w_0}{\partial t^2} + D_{15} \frac{\partial^2 w_1}{\partial t^2} \ , \tag{2.10}$$

$$A_{21} \frac{\partial^3 w_0}{\partial \varphi^3} + A_{22} \frac{\partial w_0}{\partial \varphi} + A_{23} \frac{\partial^2 v_0}{\partial \varphi^2} + A_{24} \frac{\partial^2 v_1}{\partial \varphi^2} + A_{25} \frac{\partial w_1}{\partial \varphi} + A_{26} v_1 =$$

$$= D_{21} \frac{\partial^3 w_0}{\partial \varphi \partial t^2} + D_{22} \frac{\partial^2 v_0}{\partial t^2} + D_{23} \frac{\partial^2 v_1}{\partial t^2} \ , \tag{2.11}$$

$$A_{31} \frac{\partial^2 w_0}{\partial \varphi^2} + A_{32} \frac{\partial^2 w_1}{\partial \varphi^2} + A_{33} \frac{\partial v_0}{\partial \varphi} + A_{34} \frac{\partial v_1}{\partial \varphi} + A_{35} w_0 + A_{36} w_1 = D_{31} \frac{\partial^2 w_0}{\partial t^2} + D_{32} \frac{\partial^2 w_1}{\partial t^2} \ , \tag{2.12}$$

$$A_{41} \frac{\partial^3 w_0}{\partial \varphi^3} + A_{42} \frac{\partial w_0}{\partial \varphi} + A_{43} \frac{\partial^2 v_0}{\partial \varphi^2} + A_{44} \frac{\partial^2 v_1}{\partial \varphi^2} + A_{45} \frac{\partial w_1}{\partial \varphi} =$$

$$= D_{41} \frac{\partial^3 w_0}{\partial \varphi \partial t^2} + D_{42} \frac{\partial^2 v_0}{\partial t^2} + D_{43} \frac{\partial^2 v_1}{\partial t^2} \ , \tag{2.13}$$

where A_{ij} and D_{ij} are given in the Appendix. K_{1-18} and M_{1-8} are section stiffness and mass coefficients, given by

$$K_{[1,\ldots,7]} = b \sum_{i=1}^{3} \int_{R_i}^{R_{i+1}} \frac{E_i (1 - \nu_i)}{(1 - 2\nu_i)(1 + \nu_i)} \left[1, \ r, \ \frac{1}{r}, f_i, g_i, \frac{1}{r} f_i, \frac{1}{r} g_i \right] dr \ , \tag{2.14}$$

$$K_{[8,17,18]} = b \sum_{i=1}^{3} \int_{R_i}^{R_{i+1}} G_i \left[\frac{1}{r} g_i^2, \ r \left(\frac{df_i}{dr} - \frac{f_i}{r} \right)^2, \left(\frac{df_i}{dr} - \frac{f_i}{r} \right) g_i \right] dr \ , \tag{2.15}$$

$$K_{[9,...,12]} = b \sum_{i=1}^{3} \int_{R_i}^{R_{i+1}} \frac{E_i (1 - \nu_i)}{(1 - 2\nu_i)(1 + \nu_i)} \left[\frac{1}{r} f_i^2, \frac{1}{r} g_i^2, \frac{1}{r} f_i g_i, \frac{1}{r} \left(\frac{dg_i}{dr} \right)^2 \right] dr \quad (2.16)$$

$$K_{[13,...,16]} = b \sum_{i=1}^{3} \int_{R_i}^{R_{i+1}} \frac{E_i \nu_i}{(1 - 2\nu_i)(1 + \nu_i)} \left[r \frac{dg_i}{dr}, \frac{dg_i}{dr}, f_i \frac{dg_i}{dr}, g_i \frac{dg_i}{dr} \right] dr , \quad (2.17)$$

$$M_{[1,2,3,4,5,6,7,8]} = b \sum_{i=1}^{3} \int_{R_i}^{R_{i+1}} \rho_i \left[r, \ r^2, \ r^3, \ r f_i, \ r^2 f_i, \ r f_i^2, r g_i, r g_i^2 \right] dr , \quad (2.18)$$

where $f_i = f_i(r)$ and $g_i = g_i(r)$. The kinematic and natural boundary conditions specified at $\varphi = 0$ and $\varphi = \vartheta$, are given by

KINEMATIC   NATURAL

$v_0 = 0$ or $F_{11} \frac{\partial^2 w_0}{\partial \varphi^2} + F_{12} \frac{\partial v_0}{\partial \varphi} + F_{13} \frac{\partial v_1}{\partial \varphi} + F_{14} w_0 + F_{15} w_1 = 0$,

$w_0 = 0$ or $F_{21} \frac{\partial^3 w_0}{\partial \varphi^3} + F_{22} \frac{\partial^2 v_0}{\partial \varphi^2} + F_{23} \frac{\partial^2 v_1}{\partial \varphi^2} + F_{24} \frac{\partial^3 w_0}{\partial \varphi^2 \partial t} +$

$$+ F_{25} \frac{\partial^2 v_0}{\partial t^2} + F_{26} \frac{\partial^2 v_1}{\partial t^2} = 0 , \quad (2.19)$$

$v_1 = 0$ or $F_{31} \frac{\partial^2 w_0}{\partial \varphi^2} + F_{32} \frac{\partial v_0}{\partial \varphi} + F_{33} \frac{\partial v_1}{\partial \varphi} + F_{34} w_0 + F_{35} w_1 = 0$,

$\frac{\partial w_0}{\partial \varphi} = 0$ or $F_{41} \frac{\partial^2 w_0}{\partial \varphi^2} + F_{42} \frac{\partial v_0}{\partial \varphi} + F_{43} \frac{\partial v_1}{\partial \varphi} + F_{44} w_0 + F_{45} w_1 = 0$,

$w_1 = 0$ or $F_{51} \frac{\partial w_1}{\partial \varphi} + F_{52} v_1 = 0$,

where F_{ij} are constants. For the special case of a simply supported curved band, the first, third and fourth natural boundary conditions are combined with the kinematic condition, $w_0 = w_1 = 0$.

3. Solution for a simply supported curved band

Sinusoidal mode shapes that satisfy the boundary conditions are assumed. Consequently, the assumed displacements are:

$$w_0(\varphi, t) = W_0 \cdot \sin(k_n \varphi) e^{i\omega_n t} , \quad (3.1)$$

$$w_1(\varphi, t) = W_1 \cdot \sin(k_n \varphi) e^{i\omega_n t} , \quad (3.2)$$

$$v_0(\varphi, t) = V_0 \cdot \cos(k_n \varphi) e^{i\omega_n t} , \quad (3.3)$$

$$v_1(\varphi, t) = V_1 \cdot \cos(k_n \varphi) e^{i\omega_n t} , \quad (3.4)$$

where $k_n = (n\pi)/\vartheta$. Since the motion is now harmonic, it is justified to admit hysteretic damping into the viscoelastic layer by putting complex moduli. The Young's and shear modulus of the constituent materials are represented by the complex quantities

$$E_2^* = E_2(1 + i\alpha_2), \qquad\qquad G_2^* = G_2(1 + i\beta_2) , \quad (3.5)$$

where α_2 and β_2 denote the material loss factors in extension and shear, respectively. Since G_2^* and E_2^* are used as complex moduli of the middle layer, the differential equations of motion will have complex coefficients. The substitution of equations (3.1),

(3.2), (3.3) and (3.4) into equations (2.10-2.13), will result in a set of four simulta-
neous, homogeneous algebraic equations with symmetric and complex coefficients. In
matrix form, these equations are

$$[-\omega_n^2 [M] + [Y]] \{U\} = 0, \qquad \{U\} = \{V_0, V_1, W_0, W_1\} \qquad (3.6)$$

where M_{ij} and Y_{ij} are in the Appendix. The complex eigenvalues give the desired
natural frequencies and mode shapes with their phase relations. The natural frequency
is approximately equal to the square root of the real part of the eigenvalue. The modal
loss factor for the n-th mode is approximately equal to the ratio of the imaginary part
of the eigenvalue to the real part of the eigenvalue

$$\eta_n = \text{Im}(\omega_n^2)/\text{Re}(\omega_n^2) . \qquad (3.7)$$

4. Improved estimate for shear correction functions f(r) and g(r)

An improved estimate for the correction functions $f(r)$ and $g(r)$ is derived from the
equation of elementary stress equilibrium. The equations of motion in plane strain

$$\frac{\partial}{\partial r} \left[r^2 \tau_{r\varphi} \right] + r \frac{\partial \sigma_\varphi}{\partial \varphi} = r^2 \rho \frac{\partial^2 u}{\partial t^2} , \qquad (4.1)$$

$$r \frac{\partial \sigma_r}{\partial r} + \sigma_r + \frac{\partial \tau_{r\varphi}}{\partial \varphi} - \sigma_\varphi = r\rho \frac{\partial^2 w}{\partial t^2} , \qquad (4.2)$$

applied to the layered curved band with $\sigma_{\varphi i} = E_i(\varepsilon_{\varphi i} + \nu_i \varepsilon_{ri})/\left(1 - \nu_i^2\right)$ expressions,
are now in the form

$$\frac{\partial}{\partial r}(r^2 \tau_{r\varphi i}) + \frac{E_i (1 - \nu_i)}{(1 - 2\nu_i)(1 + \nu_i)} \left[\frac{r}{R} \frac{\partial^2 v_0}{\partial \varphi^2} - \frac{r - R}{R} \frac{\partial^3 w_0}{\partial \varphi^3} + \right.$$
$$\left. + f_i(r) \frac{\partial^2 v_1}{\partial \varphi^2} + \frac{\partial w_0}{\partial \varphi} + g_i(r) \frac{\partial w_1}{\partial \varphi} \right] + r \frac{E_i \nu_i}{(1 - 2\nu_i)(1 + \nu_i)} \frac{dg_i}{dr} \frac{\partial w_1}{\partial \varphi} =$$
$$= r^2 \rho_i \left[\frac{\partial^2 v_0}{\partial t^2} - \frac{r - R}{R} \left(\frac{\partial^3 w_0}{\partial \varphi \partial t^2} - \frac{\partial^2 v_0}{\partial t^2} \right) + f_i(r) \frac{\partial^2 v_1}{\partial t^2} \right] , \quad (4.3)$$

$$r \frac{\partial \sigma_r}{\partial r} + \sigma_r - \frac{1}{r} \frac{E_i (1 - \nu_i)}{(1 - 2\nu_i)(1 + \nu_i)} \left[\frac{r}{R} \frac{\partial v_0}{\partial \varphi} - \frac{r - R}{R} \frac{\partial^2 w_0}{\partial \varphi^2} + f_i(r) \frac{\partial v_1}{\partial \varphi} + w_0 + g_i(r) w_1 \right] -$$
$$- \frac{E_i \nu_i}{(1 - 2\nu_i)(1 + \nu_i)} \frac{dg_i}{dr} w_1 + \frac{\partial \tau_{r\varphi i}}{\partial \varphi} = r\rho_i \left(\frac{\partial^2 w_0}{\partial t^2} + g_i(r) \frac{\partial^2 w_1}{\partial t^2} \right) , \qquad (4.4)$$

where $i = 1, 2, 3$ and $R_i \leq r \leq R_{i+1}$.

Using equations (2.3), (3.1), (3.2), (3.3) and (3.4), it is obvious that equations (4.3)
and (4.4) can be written the following form

$$\frac{d}{dr}(r^2 \tau_{r\varphi i}^\circ) + \frac{E_i (1 - \nu_i)}{(1 - 2\nu_i)(1 + \nu_i)} \left[-\frac{r}{R} k_n^2 V_0 + \frac{r - R}{R} k_n^3 W_0 - f_i(r) k_n^2 V_1 + \right.$$
$$\left. + k_n^2 W_0 + g_i(r) k_n^2 W_1 \right] + r \frac{E_i \nu_i}{(1 - 2\nu_i)(1 + \nu_i)} \frac{dg_i}{dr} k_n W_1 =$$

$$= -r^2 \rho_i \omega_n^2 \left[V_0 - \frac{r-R}{R} (k_n W_0 - V_0) + f_i(r) V_1 \right] , \tag{4.5}$$

$$r \frac{d\overset{\circ}{\sigma}_{ri}}{dr} + \overset{\circ}{\sigma}_{ri}(r) - \frac{1}{r} \frac{E_i(1-\nu_i)}{(1-2\nu_i)(1+\nu_i)} \left[-\frac{r}{R} k_n V_0 + \frac{r-R}{R} k_n^2 W_0 - f_i(r) k_n V_1 + \right.$$

$$\left. + W_0 + g_i(r) W_1 \right] - \frac{E_i \nu_i}{(1-2\nu_i)(1+\nu_i)} \frac{dg_i}{dr} W_1 - k_n \overset{\circ}{\tau}_{r\varphi i}(r) = -r \rho_i \omega_n^2 (W_0 + g_i(r) W_1) , \tag{4.6}$$

where $\tau_{r\varphi i}(r, \varphi, t) = \overset{\circ}{\tau}_{r\varphi i}(r) \cos(k_n \varphi) e^{i\omega_n t}$ and $\sigma_{ri}(r, \varphi, t) = \overset{\circ}{\sigma}_{ri}(r) \sin(k_n \varphi) e^{i\omega_n t}$. The shape of the shear stress distribution can be found by integrating equation (4.5) through the thickness

$$\overset{\circ}{\tau}_{r\varphi i}(r) = -\frac{1}{r^2} \int_{R_i}^{r} \left\{ r^2 \rho_i \omega_n^2 \left[V_0 - \frac{r-R}{R} (k_n W_0 - V_0) + f_i(r) V_1 \right] + \right.$$

$$\left. + r \frac{E_i \nu_i}{(1-2\nu_i)(1+\nu_i)} \frac{dg_i}{dr} k_n W_1 - \frac{E_i(1-\nu_i)}{(1-2\nu_i)(1+\nu_i)} \left[\frac{r}{R} k_n^2 V_0 - \frac{r-R}{R} k_n^3 W_0 + f_i(r) k_n^2 V_1 \right. \right.$$

$$\left. \left. - k_n^2 W_0 - g_i(r) k_n^2 W_1 \right] \right\} dr + \frac{1}{r^2} c_i , \tag{4.7}$$

where

$$c_1 = 0 , \qquad c_2 = R_2^2 \overset{\circ}{\tau}_{r\varphi 1}(R_2) , \qquad c_2 = R_3^2 \overset{\circ}{\tau}_{r\varphi 2}(R_3) . \tag{4.8}$$

Then if equation (4.7) is used in equation (4.6), the shape of the normal stress distribution can be found by integrating equation (4.6) through the thickness

$$\overset{\circ}{\sigma}_{ri}(r) = -\frac{1}{r} \int_{R_i}^{r} \left\{ r \rho_i \omega_n^2 (W_0 + g_i(r) W_1) - \frac{E_i \nu_i}{(1-2\nu_i)(1+\nu_i)} \frac{dg_i}{dr} W_1 - k_n \overset{\circ}{\tau}_{r\varphi i}(r) - \right.$$

$$\left. - \frac{1}{r} \frac{E_i(1-\nu_i)}{(1-2\nu_i)(1+\nu_i)} \left[-\frac{r}{R} k_n V_0 + \frac{r-R}{R} k_n^2 W_0 - f_i(r) k_n V_1 + W_0 + g_i(r) W_1 \right] \right\} dr + \frac{1}{r} d_i , \tag{4.9}$$

where

$$d_1 = 0 , \qquad d_2 = R_2 \overset{\circ}{\sigma}_{r1}(R_2) , \qquad d_2 = R_3 \overset{\circ}{\sigma}_{r2}(R_3) . \tag{4.10}$$

The shape of the tensile strain distribution ε_{ri} is calculated using equation (4.9) and the constitutive equation (2.5)

$$\overset{\circ}{\varepsilon}_{ri}(r) = (1 - \nu_i^2) \frac{\overset{\circ}{\sigma}_{ri}(r)}{E_i} - \nu_i \overset{\circ}{\varepsilon}_{\varphi i}(r) , \tag{4.11}$$

where $\varepsilon_{ri}(r, \varphi, t) = \overset{\circ}{\varepsilon}_{ri}(r) \sin(k_n \varphi) e^{i\omega_n t}$ and $\varepsilon_{\varphi i}(r, \varphi, t) = \overset{\circ}{\varepsilon}_{\varphi i}(r) \sin(k_n \varphi) e^{i\omega_n t}$.

Upon substitution of equation (4.11) into equation (2.4), the new estimate for the normal correction function $g(r)$ obtained by integrating equation (2.4) through the thickness, is given by

$$g_1(r) = \int_R^{R_2} \frac{1}{W_1} \overset{\circ}{\varepsilon}_{r2}(r)\, dr + \int_{R_2}^r \frac{1}{W_1} \overset{\circ}{\varepsilon}_{r1}(r)\, dr, \qquad R_1 \le r \le R_2, \qquad (4.12)$$

$$g_2(r) = \int_R^r \frac{1}{W_1} \overset{\circ}{\varepsilon}_{r2}(r)\, dr, \qquad\qquad\qquad R_2 \le r \le R_3, \qquad (4.13)$$

$$g_3(r) = \int_R^{R_3} \frac{1}{W_1} \overset{\circ}{\varepsilon}_{r2}(r)\, dr + \int_{R_3}^r \frac{1}{W_1} \overset{\circ}{\varepsilon}_{r3}(r)\, dr, \qquad R_3 \le r \le R_4. \qquad (4.14)$$

Evidently $g(R) = g_2(R) = 0$ at the reference axis.

The shape of the shear strain distribution is calculated using equation (4.7) and the constitutive relation

$$\overset{\circ}{\gamma}_{r\varphi i}(r) = \frac{\overset{\circ}{\tau}_{r\varphi i}(r)}{G_i}, \qquad\qquad i = 1, 2, 3 \qquad (4.15)$$

where $\gamma_{r\varphi i}(r, \varphi, t) = \overset{\circ}{\gamma}_{r\varphi i}(r) \cos(k_n \varphi) e^{i\omega_n t}$.

Upon substitution of equation (4.15) into equation (2.3) and using equations (4.12-4.14), the new estimate for the shear correction function $f(r)$ obtained by integrating equation (2.3) through the thickness, is given by

$$f_1(r) = r \left[\int_R^{R_2} \frac{1}{r} \left[\frac{\overset{\circ}{\gamma}_{r\varphi 2}(r)}{G} - k_n \frac{W_1 g_2(r)}{rG} \right] dr + \int_{R_2}^r \frac{1}{r} \left[\frac{\overset{\circ}{\gamma}_{r\varphi 1}(r)}{G} - k_n \frac{W_1 g_1(r)}{rG} \right] dr \right],$$
$$(4.16)$$

where $R_1 \le r \le R_2$

$$f_2(r) = r \int_R^r \frac{1}{r} \left[\frac{\overset{\circ}{\gamma}_{r\varphi 2}(r)}{G} - k_n \frac{W_1 g_2(r)}{rG} \right] dr, \qquad\qquad R_2 \le r \le R_3$$
$$(4.17)$$

and

$$f_3(r) = r \left[\int_R^{R_3} \frac{1}{r} \left[\frac{\overset{\circ}{\gamma}_{r\varphi 2}(r)}{G} - k_n \frac{W_1 g_2(r)}{rG} \right] dr + \int_{R_3}^r \frac{1}{r} \left[\frac{\overset{\circ}{\gamma}_{r\varphi 3}(r)}{G} - k_n \frac{W_1 g_3(r)}{rG} \right] dr \right]$$
$$(4.18)$$

where $R_3 \le r \le R_4$ and evidently $f(R) = f_2(R) = 0$ at the reference axis. The integrals in equations (4.7-4.18) are evaluated numerically using a trapezoidal method and $f(r)$ and $g(r)$ can be complex quantities. This new estimates of $f(r)$ and $g(r)$ are used as the correction functions for the next iteration. As with any smeared laminate model, there are two distinct ways to calculate the shear stress distribution: from the material constitutive relations; or by the elementary stress equilibrium. The ultimate goal of the iterative analysis is the determination of the functions, $f(r)$ and $g(r)$, that cause the two stress distributions to be equal. This defines the convergence point for the iterative functions $f(r)$ and $g(r)$, the point at which the stresses and strains are self-consistent.

Table 1

Variation of the lowest frequency and the loss factor with adhesive shear modulus

$G_2 \ [N/m^2]$	[20]		Present theory	
	$f \ [Hz]$	η	$f \ [Hz]$	η
$6{,}88 \cdot 10^4$	7,898	0,0644	7,508	0,0624
$6{,}88 \cdot 10^5$	11,36	0,2504	10,72	0.248
$6{,}88 \cdot 10^6$	20,94	0,1696	19,81	0.173
$6{,}88 \cdot 10^7$	25,8	0,0272	24,55	0.0281
$6{,}88 \cdot 10^8$	26,47	0,0029	25,23	0,00348

5. Results and discussion

Numerical results were generated to observe the effects of curvature, core thickness and adhesive shear modulus on the system natural frequencies ω_n and modal loss factors η_n. Vaswani et al. [20] assembled a series of design curves for the dynamic characterization of a three-layer damped circular ring segment which is simply supported at each end, see Fig.1. The model assumes that all transverse shear deformation and energy dissipation occurs in the core material. The dissipation is modeled using a complex modulus formulation. The resonant frequencies and the associated system loss factor have been experimentally determined for four sandwich beam specimens and the values compared with those obtained theoretically. Reasonably good agreement is seen between the theoretical and experimental results. However, the model of Vaswani et al. overpredicts natural frequencies by 5%, approximately. The present smeared laminate model was compared to the design curves of Vaswani et al. for the first transverse modes presented in the paper by Vaswani et al., with simply supported boundary conditions.

Table 2

Variation of the lowest frequency with adhesive thickness

$2h_2 \ [mm]$	[20]	Present theory
	$f \ [Hz]$	$f \ [Hz]$
1,0	17,981	17,028
2,0	19,1	18,125
3,0	20,09	19,04
4,0	20,94	19,81
5,0	21,66	20,47

The adhesive shear modulus plays a very important role in the damping of a sandwich curved band. The variations of the lowest natural frequency and the associated loss factor with respect to the shear modulus G_2 (= real part of G_2^*) are given in Table 1 for the three layer arch using the design curves of Vaswani et al. and the present laminate model. The input data used here were $h_1 = h_2 = h_3 = 2.0 \ mm$, $\upsilon = 1.0$, $\alpha_2 = \beta_2 = 0.5$, $R = 1.0 \ m$, $E_1 = E_3 = 6.88 \cdot 10^{10} \ N/m^2$, $G_1 = G_3 = 2.75 \cdot 10^{10} \ N/m^2$,

$\rho_1 = \rho_3 = 2.7 \cdot 10^3 \ kg/m^3$, $\rho_2 = \rho_1/2$. G_2 varied from $6.88 \cdot 10^4 \ N/m^2$ to $6.88 \cdot 10^8$ N/m^2 and $E_2 = 2.5 \cdot G_2$. The present smeared laminate model frequency predictions are generally consistent with the results of Vaswani et al. The slight discrepancy is due to facesheet shear and rotary inertia, effects which the model of Vaswani *et al.* does not consider. The model of Vaswani et al. overpredicts natural frequencies by 5%, approximately. The modal loss factors predicted by the present laminate model are also in good agreement with the results of Vaswani et al. The variation of the system loss factor η with the shear modulus G_2 is similar to that obtained for straight sandwich beams. For each core thickness, a maximum is observed which increases as the core thickness increases and is also seen to occur at higher values of the shear modulus. At low values of the shear modulus, although the deformations are large, shear stiffness is small, hence low damping is observed. At very high values of the shear modulus, the shear stiffness is high and the deformations are small, again resulting in low damping.

Table 3

Variation of the loss factor with adhesive thickness

$2h_2 \ [mm]$	[20] η	Present theory η
1,0	0,0546	0.0562
2,0	0,1	0.102
3,0	0,138	0.141
4,0	0,1696	0.173
5,0	0,196	0,199

The effects of the adhesive thickness $2h_2$ on the system natural frequencies and loss factors are also studied. The input data in this case were $h_1 = h_3 = 2.0 \ mm$, $v = 1.0$, $\alpha_2 = \beta_2 = 0.5$, $R = 1.0 \ m$, $E_1 = E_3 = 6.88 \cdot 10^{10} \ N/m^2$, $G_1 = G_3 = 2.75 \cdot 10^{10}$ N/m^2, $\rho_1 = \rho_3 = 2.7 \cdot 10^3 \ kg/m^3$, $\rho_2 = \rho_1/2$, $G_2 = 6.88 \cdot 10^4 \ N/m^2$, $E_2 = 2.5 \cdot G_2$. The thickness $2h_2$ was increased from $1.0 \ mm$ to $5.0 \ mm$ in steps of $1.0 \ mm$. The variations of f and η with $2h_2$ are given in Tables 2-3. It can be seen from these Tables that both f and η increase with $2h_2$.

Table 4

Variation of the lowest frequency with radius R

$R \ [mm]$	[20] $f \ [Hz]$	Present theory $f \ [Hz]$
800	29,75	28,1
900	24,78	23,42
1000	20,94	19,81
1100	17,9	16,95
1200	15,469	14,658

The third parameter which effects the system natural frequencies and modal loss factors is the radius of curvature R of the middle surface of the adhesive layer. In this case, the angle υ is kept constant, while changing R. This means the total length of the sandwich arch system will change with R. The variations of f and η with R are shown in Tables 4-5. The input data was $h_1 = h_2 = h_3 = 2.0\ mm$, $\upsilon = 1.0$, $\alpha_2 = \beta_2 = 0.5$, $E_1 = E_3 = 6.88 \cdot 10^{10}\ N/m^2$, $G_1 = G_3 = 2.75 \cdot 10^{10}\ N/m^2$, $\rho_1 = \rho_3 = 2.7 \cdot 10^3\ kg/m^3$, $\rho_2 = \rho_1/2$, $G_2 = 6.88 \cdot 10^4\ N/m^2$, $E_2 = 2.5 \cdot G_2$. R varied from 800 mm to 1200 mm in steps of 100 mm. It can be seen that f decreases with R. The variations of f with R are obvious, as the total length of the curved sandwich beam system increases with any increase in R.

Table 5

Variation of the loss factor with radius R.

	[20]	Present theory
$R\,[mm]$	η	$f\,[Hz]$
800	0,211	0,214
900	0,1895	0,193
1000	0,1696	0,173
1100	0,1516	0,155
1200	0,1357	0,1388

6. Conclusions

A new iterative laminate model has been presented for a thin sandwich arch that can accurately determine the dynamic stress distribution in soft as well as hard cored sandwich arches. This represents an advance over previous smeared laminate models, in which accurate estimates of the stress field were only possible if the assumed displacement field was a reasonable approximation of the actual diplacement field.

REFERENCES

1. CHIDAMPARAM, P. and LEISSA, A.W.: Vibrations of planar curved beams, rings, and arches. *Applied Mechanics Review,* **46**, (1993), 467-483.

2. LAURA, P.A.A. and MAURIZI, M.J.: Recent research on vibrations of arch-type structures. *The Shock and Vibration Digest*, **19**, (1987), 6-9.

3. MARKUS, S. and NANASI, T.: Vibrations of curved beams. *The Shock and Vibrations Digest,* **7**, (1981), 3-14.

4. DAVIS, R., HENSHELL, R.D. and WARBURTON, G.B.: Constant curvature beam finite elements for in-plane vibration. *Journal Sound and Vibrations*, **25**, (1972), 561-576.

5. AHMED, K.M.: Free vibrations of curved sandwich beams by the method of finite elements. *Journal Sound and Vibrations*, **18**, (1971), 61-74.

6. AHMED, K.M.: Dynamic analysis of sandwich beams. *Journal Sound and Vibrations*, **21**, (1972), 263-276.

7. DITARANTO, R.A.: Free and forced response of a laminated ring. *Journal of Acoustical Society of America*, **53**, (1973), 748-757.

8. LU, Y.P. AND DOUGLAS, B.E.: On the forced vibrations of three-layer damped sandwich ring. *Journal Sound and Vibrations*, **32**, (1974), 513-516.

9. SAGARTZ, M.J.: Transient response of three-layered rings. *Journal Applied Mechanics*, **44**, (1977), 299-304.

10. TATEMICHI, A., OKAZAKI, A. and HIKAYAMA, M.: Damping properties of curved sandwich beams with viscoelastic layer. *Bulletin of Nagaya Institute*, **29**, (1980), 309-317.

11. NELSON, F. C. and SULLIVAN, D.F.: The Forced vibrations of a three-layer damped circular ring. *Journal of American Society of Mechanical Engineers*, **154**, (1977), 1-8.

12. ISVAN, O. and NELSON, F. C.: Free vibrations of a three-layer damped circular ring segment. *Mecanique Materiaux Electricite,* **394-395**, (1982), 447-449.

13. KOVACS, B.: Free vibrations of a layered damped arch. *Publications of the University of Miskolc*, **36**, (1996), 65-76.

14. LIAO, C. and REDDY, J.N.: Analysis of anisotropic, stiffened composite laminates using a continuum-based shell element. *Computers and Structures*, **34**, (1990), 805-815.

15. BHIMARADDI, A., CARR, A.J. and MOSS, P.J.: Generalized finite element analysis of laminated curved beams with constant curvature. *Computers and Structures*, **31**, (1989), 309-317.

16. QATU, M.S.: In-plane vibration of slightly curved laminated composite beams. *Journal of Sound and Vibrations,* **159**, (1992), 327-338.

17. QATU, M.S. and ELSHARKAWY, A.A.: Vibration of laminated composite arches with deep curvature and arbitrary boundaries. *Computers and Structures*, **47**, (1993), 305-311.

18. QATU, M.S.: Equations for the analysis of thin and moderately thick laminated composite curved beams. *International Journal of Solid and Structures*, **30**, (1992), 2743-2756.

19. YILDIRIM, V.: Rotary inertia, axial and shear deformation effects on the in-plane natural frequencies of symmetric cross-ply laminated circular arches. *Journal of Sound and Vibration*, **224**, (1999), 575-589.

20. VASWANI, J., ASNANI, N.T. and NAKRA, B.C.: Vibration and damping analysis of curved sandwich beams with a viscoelastic core. *Composite sturctures*, **10**, (1988), 231-245.

21. HE, S. and RAO, M.D.: Prediction of loss factors of curved sandwich beams. *Journal of Sound and Vibration*, **159**, (1992), 101-113.

22. ZAPFE, J. A. and LESIEUTRE, G. A.: Vibration analysis of laminated beams using an iterative smeared laminate model. *Journal of Sound and Vibration*, **199**, (1997), 275-284.

23. KOVACS, B., SZABO, F.J. and DOBROCZONI, A.: Free vibrations of a layered circular ring segment. *microCAD-SYSTEM '93 International Computer Science Meeting Proceding,* Miskolc, Hungary, (1993), 65-77.

24. KOVACS, B.: *Vibration and stability of layered circular arch,* Ph.D. thesis, Hungarian Academy of Sciences, Budapest, (1992). (in Hungarian)

25. ROSSETTOS, J.N.: Vibration of slightly curved beams of transversely isotropic composite materials. *American Institute of Aeronautics and Astronautic Journal,* **9**, (1971), 2273-2275.

26. ROSSETTOS, J.N. and SQUIRES, D.C.: Modes and frequencies of transversely isotropic slightly curved Timoshenko beams. *Journal of Applied Mechanics*, **40**, (1973), 1029-1033.

27. KHDEIR, A.A. and REDDY, J.N.: Free and forced vibration of cross-ply laminated composite shallow arches. *International Journal of Solids and Structures*, **34**, (1997), 1217-1234.

28. YILDIRIM, V. : Out-of-plane free vibration characteristics of symmetric cross-ply laminated composite arches with deep curvature. *Journal of the Mechanical Behavior of Materials,* **10**, (1999), 165-186.

Appendix A. NOMENCLATURE

b	width of the curved band
E_i	elastic modulus of layer i
E_2^*	complex modulus in tension
$\mathbf{e}_r$	unit vector in the radial direction
$\mathbf{e}_\varphi$	unit vector in the transverse direction
$\mathbf{e}_z$	unit vector in the z-direction
$\varepsilon_{\varphi i}$	tensile strain of layer i in the transverse direction
ε_{ri}	tensile strain of layer i in the radial direction
$f(r)$	shear correction function
$g(r)$	normal correction function
$\gamma_{r\varphi i}$	shear strain of layer i
G_2^*	complex modulus in shear
G_i	shear modulus of layer i
h_i	half-thickness of layer i
φ	circumferential coordinate
n	mode number
r	cylindrical coordinate
R	radius of middle surface of the curved band
T	kinetic energy
$\sigma_{\varphi i}$	tensile stress of layer i in the transverse direction
$\sigma_{r i}$	tensile stress of layer i in the radial direction
$\tau_{r\varphi i}$	shear stress of layer i
$\mathbf{t}_i$	displacement vector of layer i
R_1	radius at the bottom of the first layer
R_2	radius at the top of the first layer
R_3	radius at the bottom of the third layer
R_4	radius at the top of the third layer
α_2	material loss factor in tension of the second layer
β_2	material loss factor in shear of the second layer
η_n	composite loss factor for the n-th mode
ω_n	frequency of oscillation in radians for the n-th mode
f_n	frequency of oscillation in Hertz for the n-th mode
ρ_i	density of layer i

ϑ	opening angle of the curved band
v_0	tangential displacement of the middle surface
w_0	radial displacement of the middle surface

Appendix B. Definitions for the various coefficients

Equations (2.10) to (2.13) in the main text contain certain A_{ij} and D_{ij} terms which are defined as follows:

$$A_{11} = K_3 + K_2/R^2 - 2K_1/R, \quad A_{12} = 2K_3 - 2K_1/R, \quad A_{13} = -K_2/R^2 + K_1/R$$

$$A_{14} = K_6 - K_4/R, \quad A_{15} = K_1/R, \quad A_{16} = K_6, \quad A_{17} = K_{14} + K_7 - K_{13}/R - K_5/R$$

$$A_{18} = K_3, \quad A_{19} = K_{14} + K_7, \quad A_{21} = K_4/R - K_6, \quad A_{22} = -K_6, \quad A_{23} = -K_4/R,$$

$$A_{24} = -K_9, \quad A_{25} = K_{18} - K_{15} - K_{11}, \quad A_{26} = K_{17}$$

$$A_{31} = -K_{13}/R + K_{14} - K_5/R + K_7, \quad A_{32} = -K_8, \quad A_{33} = K_{13}/R + K_5/R$$

$$A_{34} = K_{15} + K_{11} - K_{18}, \quad A_{35} = K_7 + K_{14}, \quad A_{36} = K_{12} + 2K_{16} + K_{10}$$

$$A_{41} = K_2/R^2 - K_1/R, \quad A_{42} = -K_1/R, \quad A_{43} = -K_2/R^2, \quad A_{44} = -K_4/R$$

$$A_{45} = -K_{13}/R - K_5/R$$

$$D_{11} = M_1 - 2M_2/R + M_3/R^2, \quad D_{12} = M_2/R - M_3/R^2, \quad D_{13} = M_4 - M_5/R$$

$$D_{14} = -M_1, \quad D_{15} = -M_7, \quad D_{21} = -M_4 + M_5/R, \quad D_{22} = -M_5/R$$

$$D_{23} = -M_6, \quad D_{31} = -M_7, \quad D_{32} = -M_8, \quad D_{41} = -M_2/R + M_3/R^2$$

$$D_{42} = -M_3/R^2, \quad D_{43} = -M_5/R.$$

Equation (3.6) in the main text contain Y_{ij} and M_{ij} terms which are defined as follows:

$$Y_{11} = \left(2k_n^2 - 2k_n^4\right) K_1/R + k_n^4 K_2/R^2 + \left(1 - 2k_n^2 + k_n^4\right) K_3$$

$$Y_{12} = Y_{21} = -k_n K_6 + k_n^3 \left(K_6 - K_4/R\right),$$

$$Y_{14} = Y_{41} = -k_n K_1/R + k_n^3 \left(K_1/R - K_2/R^2\right),$$

$$Y_{13} = Y_{31} = K_{14} + K_7 - k_n^2 \left(K_{14} + K_7 - K_{13}/R - K_5/R\right), \quad Y_{22} = K_{17} + k_n^2 K_9$$

$$Y_{23} = Y_{32} = k_n \left(K_{18} - K_{15} - K_{11}\right), \quad Y_{24} = Y_{42} = k_n^2 K_4/R, \quad Y_{44} = k_n^2 K_2/R^2$$

$$Y_{33} = K_{12} + 2K_{16} + K_{10} + k_n^2 K_8, \quad Y_{34} = Y_{43} = -k_n \left(K_{13}/R + K_5/R\right)$$

$$M_{11} = M_1 + k_n^2 \left(M_1 + M_3/R^2 - 2M_2/R\right), \quad M_{12} = M_{21} = k_n \left(M_4 - M_5/R\right)$$

$$M_{13} = M_{31} = M_7, \quad M_{14} = M_{41} = k_n \left(M_2/R - M_3/R^2\right), \quad M_{22} = M_6$$

$$M_{24} = M_{42} = M_5/R, \quad M_{33} = M_8, \quad M_{44} = M_3/R^2$$

$$M_{23} = M_{32} = M_{24} = M_{42} = 0.$$